Iran J Sci Technol Trans Sci (2021) 45:2191–2199
https://doi.org/10.1007/s40995-021-01210-4

RESEARCH PAPER

Effects of Aging on Magnetic and Thermal Characteristics of NiMnCoSn Magnetic Shape Memory Alloys

Mediha Kök[1] · Kumruya Aydoğdu[1] · M. Sait Kanca[2] · Ibrahim Nazem Qader[3] · Ecem Öner[1] · Meltem Coşkun[1]

Received: 6 May 2021 / Accepted: 15 August 2021 / Published online: 21 August 2021

Abstract

Heusler shape memory alloys are important for many applications due to their typical magnetic and shape memory behaviors. In this study, a $Ni_{50}Mn_{36}Sn_{12}Co_2$ (at.%) alloy was manufactured by arc-melting technique, then the ingot cooled to ambient temperature in the natural atmosphere. Three different temperatures, including 500 °C (773 K), 700 °C (973 K), and 900 °C (1173 K), was selected for aging the samples cut from the main ingot. The impact of aging on the crystalline; microstructure; caloric; and magnetic properties of the alloys were investigated through x-ray diffraction (XRD); scanning electron microscope; differential scanning calorimetric (DSC), differential thermal analysis, and thermal gravimetric (TG); and physical property measuring system was investigated, respectively. The aging in different temperatures led to the shift DSC curve, such that the martensitic phase transformation temperatures of the sample aged at 773 K increased, however, the transformation at 973 and 1173 K decreased compared to the as-casted alloy. The different phase transformation behavior showed that the alloy aged at 773 K has the maximum elastic energy, enthalpy and entropy change compared to the reset of samples, on the other hand, its crystallite sized obtained from XRD analysis comparably diminished. Besides, the TG analysis revealed that the mass gain almost occurs at a temperature above 773 K, therefore the magnetization of the alloys aged at 973 and 1173 K decreased due to a thin oxide layer formed on the surface of the alloys.

Keywords NiMnCoSn · Magnetic shape memory alloy · Aging · Thermal characteristics · XRD · Microstructure

1 Introduction

Magnetic shape memory alloys (MSMAs) are smart materials that show shape change not only thermally, but also by the applied magnetic field (Fukushima et al. 2009; Liu et al. 2017). The MSMAs are the best well-known Heusler alloys, which historically began in 1903 with the discovery of Cu-Al-Mn alloys by Fritz Heusler (Bachaga et al. 2019). The crystal structure of MSMAs can switch between the austenite and martensite phases due to the response to an external magnetic field (Yang et al. 2016). In recent years, this unique alloy capability has been in demand in various applications. They are especially used in actuator and sensor applications. The MSMAs are divided into two types according to their operating mechanism. These alloys exhibit a magnetic shape memory effect resulting from the rearrangement of martensitic variants, which the magnetic shape memory effect (MSME) can reach up to 10%, however, the blocking stress is quite low

✉ Ibrahim Nazem Qader
inqader@gmail.com

Mediha Kök
msoglu@firat.edu.tr

M. Sait Kanca
msaitkanca23@gmail.com

Ecem Öner
ecemozen92@gmail.com

Meltem Coşkun
meltemcoskun231991@gmail.com

[1] Department of Physics, Faculty of Science, Firat University, Elazig, Turkey

[2] Rare Earth Elements Application and Research Center (MUNTEAM), Munzur University, Tunceli, Turkey

[3] Department of Physics, College of Science, University of Raparin, Sulaymaneyah, Iraq

(Cong et al. 2010). High output stress levels and relatively large MSME make these alloys extremely attractive (Castillo-Villa et al. 2013; Kamila 2013; Qu et al. 2018).

The MSMAs were more widely investigated after the discovery of the magnetic field effect martensitic transformation in NiMn- (In, Sn, Sb) alloys by Sutou et al. in 2004 (Sutou et al. 2004). Kaunima et al. determined that the NiCoMnIn and NiCoMnSn polycrystalline alloys exhibit strain recovery through martensitic phase transformation (Kainuma et al. 2006a, b; Kainuma et al. 2006a, b). Among these MSMAs, NiCoMnIn alloys have been studied most extensively, however, NiCoMnSn alloys are also highly promising for practical applications because they contain no expensive elements (Ito et al. 2007; Khovaylo et al. 2010; Mañosa et al. 2008). For example, it is reported that raising the cobalt content of nitinol increases the number of martensite planes and, as a result, the value of transformation temperatures (N. El-Bagoury 2014). El-Bagoury et al. improved corrosion resistance of $Ni_{52}Ti_{48-x}Co_x$ (wt%) SMAs (Nader El-Bagoury et al. 2013). Besides, Alqarni et al. obtained the same results by adding Co into a NiTi (Alqarni et al. 2018).

Ito et al. studied Ni-Mn-In, Ni-Co-Mn-In, and Ni-Co-Mn-Sn Heusler alloy systems and found that these SMAs had two different magnetic behaviors, whereby at the higher temperature they have ferromagnetic parent phase, while at lower temperatures, they have paramagnetic martensite phase. They confirmed that the magnetic field induced inverse martensitic transformation (Ito et al. 2007). The NiMnCoSn alloy system has many advantages, such as non-toxic elements, inexpensive elements, and easy manufacturing.

Along with these, MSMAs have a high magnetocaloric effect and magneto-resistance (GschneidnerJr et al. 2005; Huang et al. 2015; Zimm et al. 1998). By applying a magnetic field, the magnetic entropy value of the materials decreases, thus, the heat spreads isothermally from the magnetic cooling system to the environment. When the external magnetic field is removed, an opposite phenomenon can be observed, such that the magnetic entropy increases, and therefore, the material absorbs heat energy from the environment. This effect is called the magnetocaloric effect. The magnetocaloric effect is defined as the intrinsic property of a magnetic material (Shen et al. 2009; Zimm et al. 1998). There are many MSMAs, however, the Ni–Mn–Ga is one of the most studied alloys. The Substitution of Ga with Sn is an economic alternative for Ni–Mn–Ga alloys. For this, many studies have been carried out recently on the development of NiMnSn and NiMnSn-based alloys (Khalil-Allafi et al. 2002; Medika Kök et al. 2019a, b, c).

This study aims to improve the properties of NiMnCoSn high temperature shape memory alloy by heat treatment. For this purpose, three high temperatures were used for aging the quaternary NiMnCoSn alloy to investigate caloric feature, crystal structure, and magnetic behavior. Additionally, some theoretical calculations were performed to investigate the impact of aging on the different characteristics of the alloy.

2 Experimental Procedure

A quaternary $Ni_{50}Mn_{36}Sn_{12}Co_2$ (at.%) magnetic shape memory alloy was produced using an arc-melter in a controlled atmosphere. The alloy was aged at 773, 973, and 1173 K for 1 h; the corresponding alloys were labeled as NMCS1, NMCS2, and NMCS3, respectively, also the as-received alloy was labeled as NMCS0. The TG/DTA measurements were made at room temperature up to 1273 K for as-received $Ni_{50}Mn_{36}Sn_{12}Co_2$ (at.%) magnetic shape memory. The results were used for determining the high-temperature behavior of the alloy and to choose the ideal heat treatment temperatures.

Figure 1 shows that there is no change in the DTA and TG curves of the sample up to 530 °C, which is indicated as the "change point", while after 530 °C there is a flat peak in the heat flux curve and a rapid mass increase in the TG curve. Based on this curve, the mass removal and the temperature of 500 °C (before a new phase transformation) and the temperature at which this transformation started (700 and 900 °C) were chosen as the heat treatment temperatures. After the aging process, the crystal structure analysis of heat-treated NiMnSnCo alloys was performed at room temperature with a Rigaku brand x-ray diffractometer with a scan rate of 6°/min. The microstructures and elemental chemical analysis of the same alloys were determined by SEM–EDX (scanning electron microscope – energy dispersive x-ray analysis). The martensitic phase transformation temperatures of non-heat-treated and heat-treated alloys were measured with the heating–cooling rate of 10 °C/min using a Perkin Elmer differential scanning calorimeter (DSC) in nitrogen gas atmosphere. Finally, to investigate the effect of heat treatment on the magnetic properties of NiMnSnCo alloy, room temperature magnetization measurement was made using Quantum PPMS (physical property measuring system) device in the magnetic field range of − 5 T to 5 T.

3 Results and Discussions

Figure 2 displays complete heating and cooling DSC curves of the main and heat-treated samples taken between 223 and 423 K. Besides, the value of A_s (austenite start), A_p (austenite peak), A_f (austenite finish), M_s (martensite start),

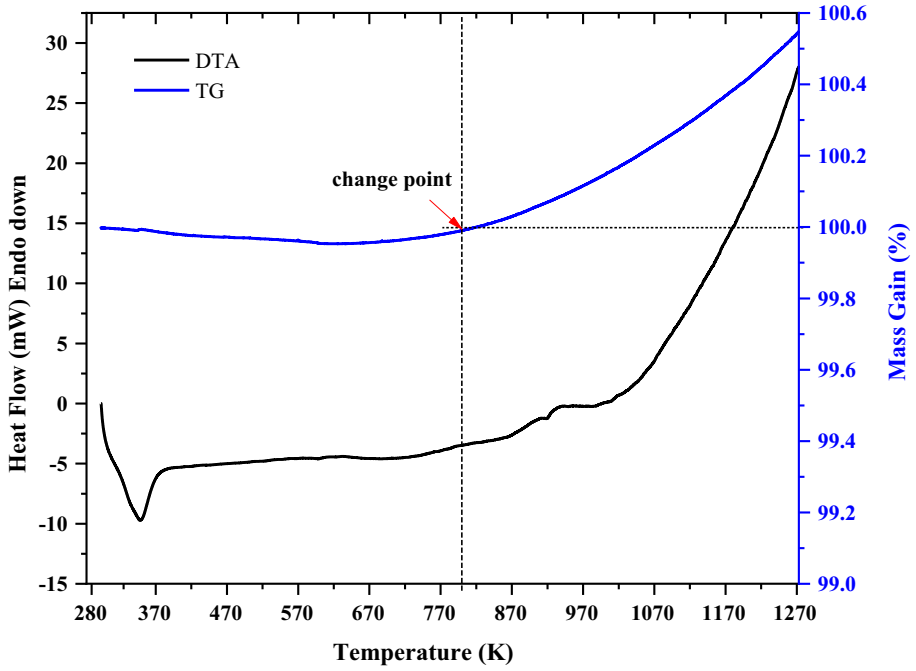

Fig. 1 The DTA and TG of the as-received and aged NiMnCoSn alloys

M_p (martensite peak), M_f (martensite finish), and the enthalpy changes ($\Delta H_{heating}$ and $\Delta H_{cooling}$) are given in Table 1. In the temperature-varying heat flux curve of NMCS0, a multiple phase change was observed during the austenite transformation (indicated by an arrow in Fig. 2). During both austenite and martensite transformation, it is noticed that the transformation energies are low and the peaks were broad. Similarly, it was observed the multi-phase during austenite transformation and the single-phase during martensite transformation in the NMCS1. It was observed that the multiple phases disappeared at the alloy heat-treated at 973 K and 1173 K. When the transformation temperatures in Table 1 are examined, a serious decrease has been observed in the martensitic transformation temperatures with the increase of the heat treatment temperature.

Figure 3 and 4 show the XRD patterns and the SEM micro-images of the as-casted and aged NiMnCoSn alloy, moreover the composition of the entire surface of the as-received alloy is given Fig. 4e. There is no sign of pour or micro-cracks on the surface of the alloys. The XRD measurements were performed to determine the crystal structure and to specify matrix and second phases. On the other hand, SEM images show a larger view of the microstructures. The main difference between these two measurements was the sample preparation. Although both measurements were carried out at room temperature, the surface of the samples was grinded, smoothed, and finally etched for accomplishing the SEM technique, while after the aging process, no further modification was done on the surface of the alloys for the XRD measurements. Therefore, the SEM images give information about microstructures, such as twinned martensite (the inset of Fig. 4e), whereas the XRD patterns reveal the formation of second phases on the surface during aging in high temperatures.

The XRD peaks were indexed by the literature (Chen et al. 2014; Elwindari et al. 2017; Mishra et al. 2015). In this study, XRD diffractograms show the characteristic peaks corresponding to the parent, martensite, and second phases of the NiMnCoSn Magnetic shape memory alloy. The NMCS3 aged at 900 °C (1173 K) has denser and sharper peaks compared to the other samples, which indicated new phases, such as oxides and other compounds formed at the higher temperature. Normally, the probability of forming an oxide layer and producing compounds from the constituents is increased with increasing temperature at elevated temperatures. Also, in high temperatures, normally some compounds get enough activation energy to form. In the current study, the alloy starts to mass gain at temperatures higher than 500 °C (773 K), thus the second phases increased by increasing aging temperature. The existing second phase, especially the oxidation film on the surface, can influence alloy characterizations, such as magnetic property (Kök et al. 2013).

To explore caloric properties of the alloys, thermodynamics parameters, such as enthalpy change, entropy

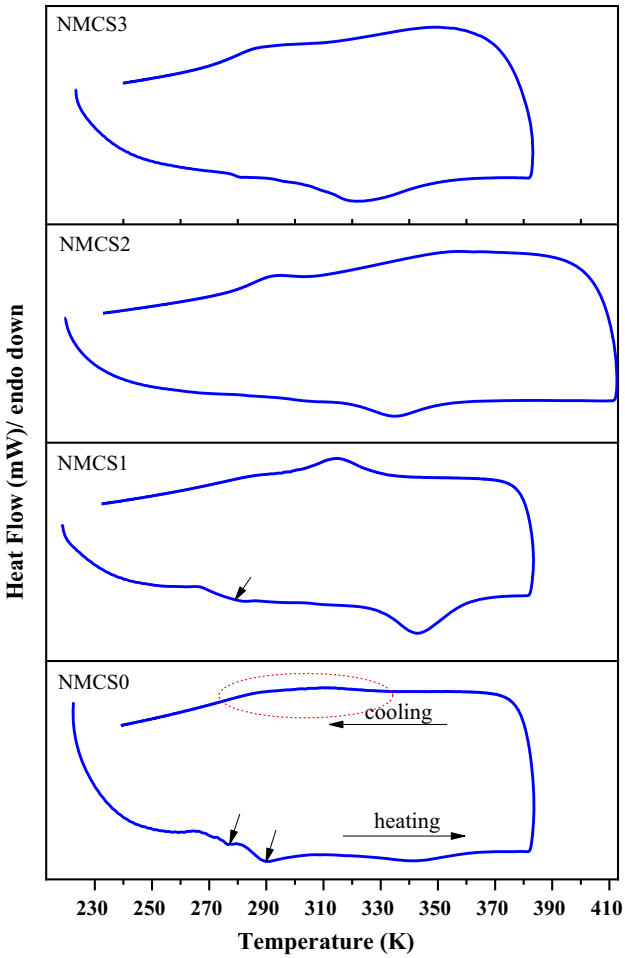

Fig. 2 The DSC curves of the as-received and aged NiMnCoSn alloys, where NMCS0 is as-received alloy; NMCS1, NMCS2, and NMCS3 are codes for the aged alloys at 773, 973, and 1173 K for 1 h, respectively

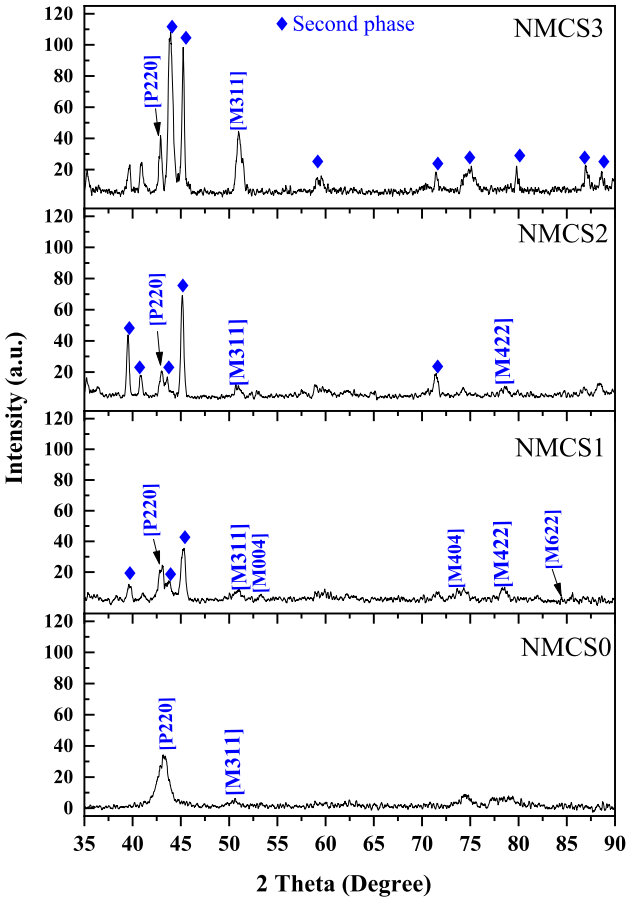

Fig. 3 X-ray diffraction pattern of the alloys obtained at room temperature

change, and elastic energy was calculated by using analyzing the DSC results. The temperature hysteresis was calculated by subtracting A_p and M_p (Dagdelen et al. 2020; Qader et al. 2020a, b, c):

$$\text{Temperature hysteresis} = A_p - M_p \tag{1}$$

Also, to find the thermally induced entropy change (ΔS) during martensite (M) to austenite (A) phase transformation, the following equation was utilized (Dagdelen et al. 2019; Qader et al. 2020a, b, c; Tatar and Yildirim 2017):

$$\Delta S^{M\to A} = \int_{A_s}^{A_f} \frac{dQ^{M\to A}}{T_o} = \frac{\Delta H^{M\to A}}{T_o} \tag{2}$$

Here T_o is the temperature where the Gibbs free energy for forward and reverse phase transformation is equal to zero, thus it is called equilibrium temperature and its value can be found by the average value of martensite start and austenite finish temperatures (Ercan et al. 2020; Mohammed et al. 2020):

$$T_o = (M_s + A_f)/2 \tag{3}$$

Table 1 The phase transformation temperatures and enthalpy changes of the phase transformation of the as-received and aged NiMnCoSn alloys

Sample's code	A_s (K)	A_p (K)	A_f (K)	M_s (K)	M_p (K)	M_f (K)	$\Delta H_{heating}$ (J/g)	$\Delta H_{cooling}$ (J/g)	$\Delta H_{average}$ (J/g)
NMCS0	337.1	353.1	380.1	325	309.5	296	0.91	2.77	1.84
NMCS1	328.2	343.3	362.2	332.6	315	298	4.72	4.54	4.63
NMCS2	321.9	335	353.6	306.9	293.1	278.8	4.83	3.14	3.99
NMCS3	303	322.4	352.1	308.6	286.8	270.5	5.47	1.60	3.53

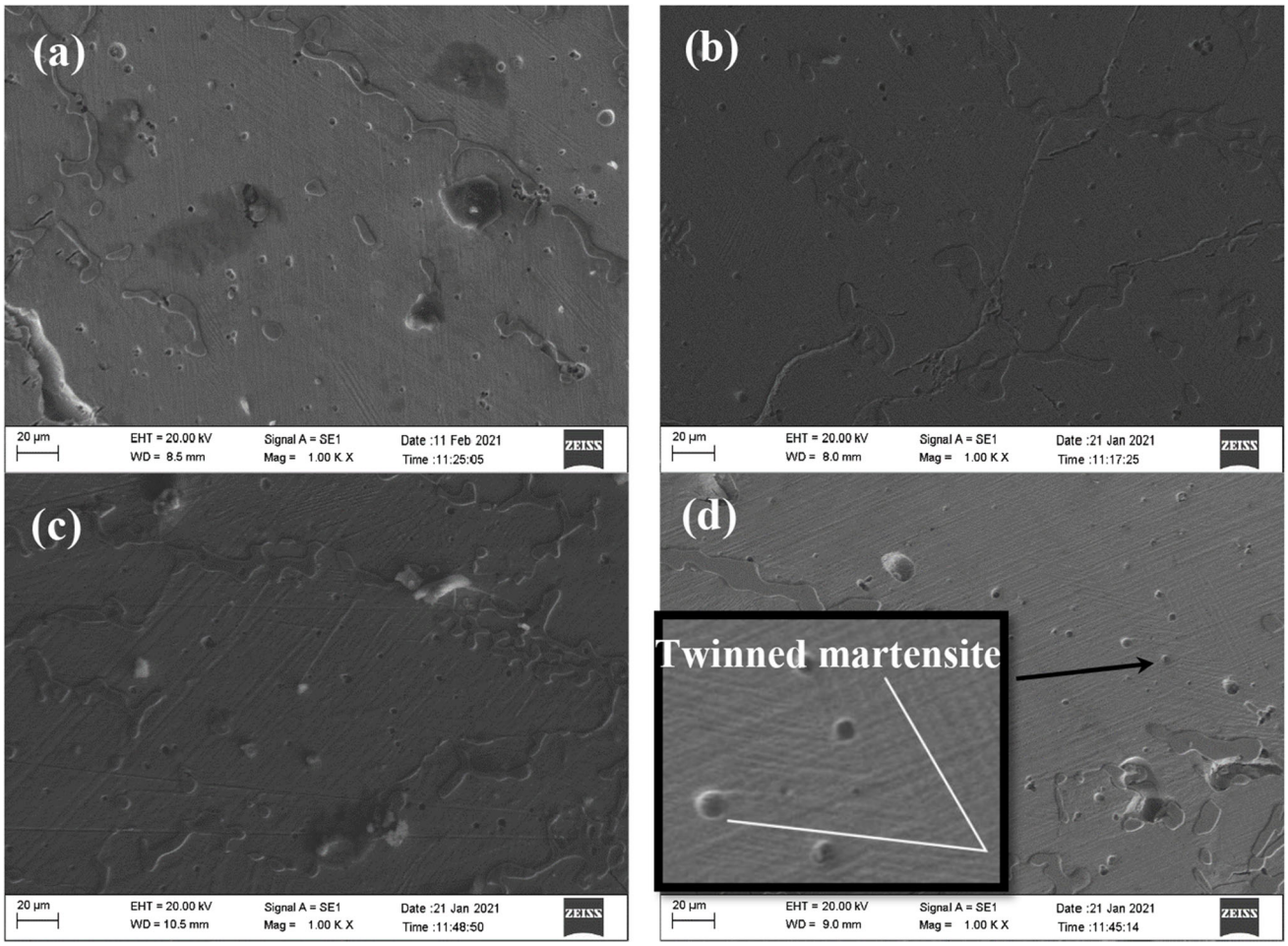

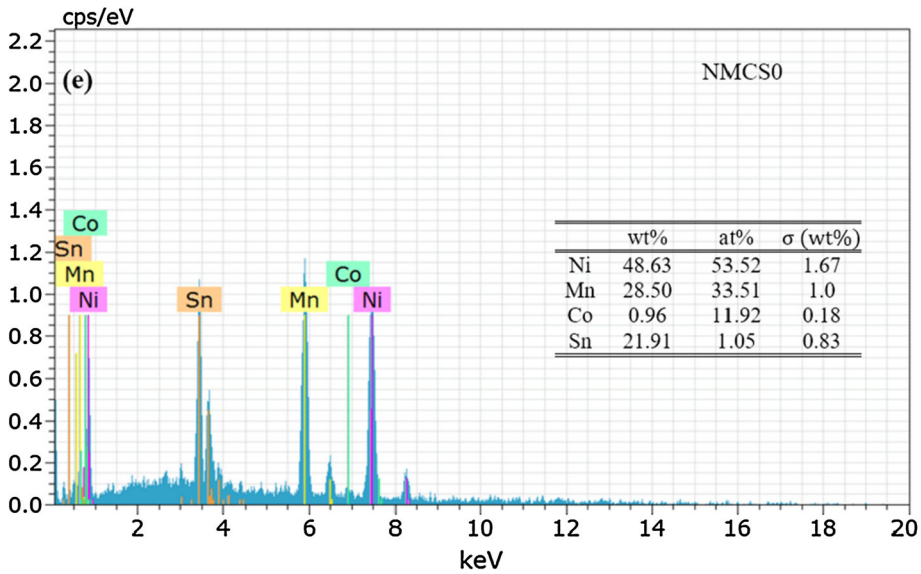

Fig. 4 The SEM images taken at room temperature for the **a** as-received and aged NiMnCoSn alloys at **b** 773 K, **c** 973 K, and **d** 1173 K; The EDS of the entire surface of the as-received alloy

In Eq. (1), ΔH is the enthalpy change of the austenite phase transformation. Its value normally can be obtained using software, such as Origin program, through finding the area under austenite phase transformation from A_s to A_f (Mediha Kök et al. 2019a, b, c; Qader et al. 2020a, b, c):

$$\Delta H^{M\to A} = \int_{A_s}^{A_f} \frac{dq}{dt}\left(\frac{dT}{dt}\right)^{-1} dT \tag{4}$$

The Gibbs free energy (ΔG), as a thermodynamics parameter, was found using subtracting equilibrium temperature from martensite start and the value of $\Delta S^{M\to A}$ obtained from Eq. (2) (Mediha Kök et al. 2019a, b, c):

$$\Delta G^{A\to M}(M_s) = -(T_o - M_s)\Delta S^{M\to A} \tag{5}$$

Elastic energy (ΔE_e) is the energy stored in martensite variants (Balci et al. 2021; Tatar and Yildirim 2017). The ΔE_e primarily consists of elastic strain energy that is either stored or lost as a result of lattice distortion when forming or transforming martensite variants. Since some energy is consumed due to frictional resistance during the shear motion of the boundary, it causes various structural defects, and a small part of it is lost when the sound wave propagates, so this process is not reversible (Otsuka and Wayman 1999). The elastic energy for reverse phase transformation was calculated by (Acar et al. 2020; Kök et al. 2020; Qader et al. 2019):

$$\Delta E_e = \left(M_s - M_f\right)\Delta S^{M\to A} \tag{6}$$

Other information extracted from the XRD pattern is the crystal size (D) of the alloys obtained using the Scherrer equation (Tatar et al. 2020) that depends on some parameters, including, wideness at half maximum (FWHM), Bragg's angle (θ), the wavelength of the x-ray source (λ). The Scherrer equation is as follows (Mediha Kök et al. 2019a, b, c):

$$D = K\lambda/(B\cos\theta) \tag{7}$$

where B is the FWHM obtained by X-Pert High Score Plus, the shape factor is chosen as (K = 0.9), and $\lambda_{K_\alpha}(Cu)$ with a wavelength of 1.5406 Å was used in the XRD measurements.

The enthalpy change of austenite and martensite phase transformations are listed in Table 1. Also, the temperature hysteresis, entropy change of martensite phase transformation, equilibrium temperature, Gibbs free energy for the forward phase transformation, and elastic energy was calculated by using Eqs. (1), (2), (3), (5), and (6), respectively. Table 2 lists the aforementioned parameters. Figure 5 displays the calculated parameters to compare them for the investigated samples. The NMCS0 sample has the maximum value of the average ΔH for a complete thermal cycle, entropy change, and elastic energy compared to the other alloys. On the other hand, NMCS0 has the lowest crystallite size that calculated using XRD measured at room temperature.

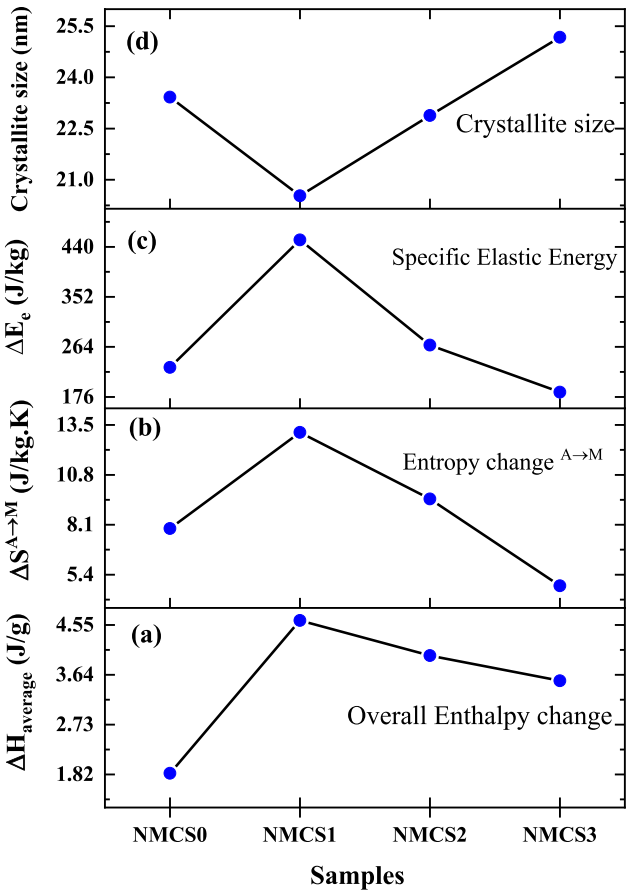

Fig. 5 Calculated parameters; **a** average enthalpy and **b** entropy change of martensite phase transformation; **c** elastic energy; **d** crystallite size

Almost all parameters supported the magnetic behavior of the Huesler alloys. Magnetic properties of a shape

Table 2 The calculated parameters of the as-received and aged NiMnCoSn alloys

Sample's code	A_p-M_p (K)	T_o (K)	$\Delta S_{A\text{-}M}$ (J/kg.K)	G_E (J/kg)	$\Delta G_{A\text{-}M}$ (J/kg)
NMCS0	43.6	352.6	7.9	227.9	71.1
NMCS1	28.3	347.4	13.1	452.2	201.1
NMCS2	41.9	330.3	9.5	267.2	341.5
NMCS3	35.6	330.4	4.8	184.5	360.1

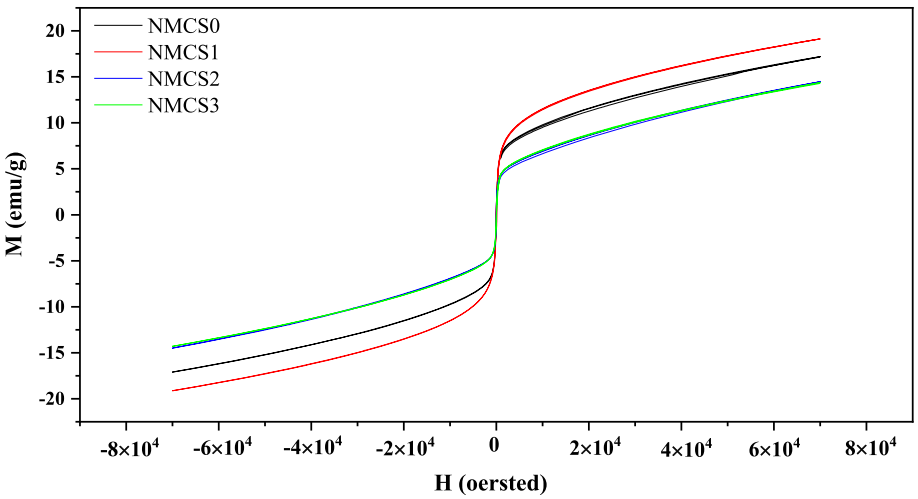

Fig. 6 **a** The magnetization behavior and **b** the calculated crystallite size of the as-received and aged NiMnCoSn alloys

memory alloy strongly depend on the matrix phase (Bruno et al. 2018; Lázpita et al. 2016). Figure 6 shows the magnetization curves of the NiMnSnCo alloy at room temperature before and after heat treatment. In these curves, the applied external magnetic field and the change in the magnetic field within the alloys can be observed. The magnetic property of the NiMnSnCo alloy shows different characteristics after heat treatment at 773 K. Similar effects can be observed in the thermal analysis of the as-casted and aged Heusler alloys. Normally, the grain size increases with the aging, therefore, the resistance of the domain walls to the magnetic dipole motions decreases with the increase of the grain size, so it is expected that the magnetization will increase (Dong and Gao 2016; Li et al. 2018; Öztürk et al. 2020). On the other hand, although the magnetization value of the alloy increased at 773 K, it diminished with increasing aging temperatures. While the temperature increased the magnetic saturation point at 773 K, however a thin oxide layer formed after aging the alloy at a temperature greater than 773 K, since the TG result in Fig. 1 showed that the mass gain (i.e., oxidation) starts at a temperature above 773 K. As a result, after aging at 973 K and 1173 K, an oxide layer formed on the surface of the NiMnCoSn alloy, thus, due to oxide formation, the amount of magnetic saturation value diminished, which is also supported by the reported articles. Regarding the oxidation process on a ternary NiMnGa alloy, Kök et al. stated that the magnetic saturation decreased as a result of oxidation at high-temperature, whereby the reason was the increase in the amount of oxide on the alloy (Kök et al. 2013).

4 Conclusion

This study aimed to investigate caloric, crystal structure, and magnetic behavior of a quaternary NiMnCoSn magnetic shape memory alloy. Three different temperatures were selected based on DTA/TG results. The aging at 773 K enhanced the magnetization of the alloy while increasing the aging temperature to 973 and 1173 K diminished the magnetic behavior of the Heusler alloy. Additionally, the crystallite size calculated by the Scherrer equation decreased from 23.4 nm to 30.5 nm by aging the NiMnCoSn alloy, while it increased with increasing aging temperature. On the other hand, the heat treatment affected the caloric properties of the alloy, whereby the DSC curves show different phase transformation temperatures. Additionally, the entropy change, enthalpy change, and specific elastic energy of the NMCS1 aged at 773 K recorded the maximum values compared to the as-received alloy, NMCS2, and NMCS3 alloys. Consequently, by using a prior DTA/TG measurement, an optimum aging temperature was found for aging the $Ni_{50}Mn_{36}Sn_{12}Co_2$ alloy.

Author's Contribution M. KOK main idea and experimental. N. QADER and A. I. HAJI have performed all calculations and analysis. Kumruya AYDOĞDU, Sait KANCA, and Meltem COŞKUN literature review. Ibrahim Nazem QADER, and Ecem ÖNER discussion and data analysis. Additionally, all authors contributed to writing and approved the final manuscript.

Funding This work was supported by the Management Unit of the Scientific Research Projects of Firat University (FUBAP) (Project Numbers: FF.20.02 & 20.06).

Data availability statement The data associated with a paper is available, and under what conditions the data can be accessed.

Declarations

Conflict of interest The authors state that there is no conflict of interest in the printing of this manuscript.

Consent to Publish The Authors hereby consents to publication of the Work in "Iranian Journal of Science and Technology, Transaction A, Science (ISTT)"

References

Acar E, Kok M, Qader IN (2020) Exploring surface oxidation behavior of NiTi–V alloys. Eur Phys J plus 135:58. https://doi.org/10.1140/epjp/s13360-019-00087-y

Alqarni ND, Wysocka J, El-Bagoury N, Ryl J, Amin MA, Boukherroub R (2018) Effect of cobalt addition on the corrosion behavior of near equiatomic NiTi shape memory alloy in normal saline solution: Electrochemical and XPS studies. RSC Adv 8:19289–19300. https://doi.org/10.1039/C8RA02031K

Bachaga T, Zhang J, Khitouni M, Sunol JJ (2019) NiMn-based Heusler magnetic shape memory alloys: a review. Int J Adv Manuf Technol 103:2761–2772. https://doi.org/10.1007/s00170-019-03534-3

Balci E, Dagdelen F, Qader IN, Kok M (2021) Effects of substituting Nb with V on thermal analysis and biocompatibility assessment of quaternary NiTiNbV SMA. Eur Phys J plus 136:145. https://doi.org/10.1140/epjp/s13360-021-01149-w

Bruno NM, Salas D, Wang S, Roshchin IV, Santamarta R, Arroyave R, Duong T, Chumlyakov YI et al (2018) On the microstructural origins of martensitic transformation arrest in a NiCoMnIn magnetic shape memory alloy. Acta Mater 142:95–106. https://doi.org/10.1016/j.actamat.2017.08.037

Castillo-Villa PO, Mañosa L, Planes A, Soto-Parra DE, Sánchez-Llamazares JL, Flores-Zúñiga H, Frontera C (2013) Elastocaloric and magnetocaloric effects in Ni–Mn–Sn(Cu) shape-memory alloy. J Appl Phys 113:053506. https://doi.org/10.1063/1.4790140

Chen F, Tong Y-X, Tian B, Li L, Zheng Y-F (2014) Martensitic transformation and magnetic properties of Ti-doped NiCoMnSn shape memory alloy. Rare Met 33:511–515. https://doi.org/10.1007/s12598-013-0100-7

Cong DY, Roth S, Pötschke M, Hürrich C, Schultz L (2010) Phase diagram and composition optimization for magnetic shape memory effect in Ni–Co–Mn–Sn alloys. Appl Phys Lett 97:021908. https://doi.org/10.1063/1.3454239

Dagdelen F, Kok M, Qader IN (2019) Effects of Ta content on thermodynamic properties and transformation temperatures of shape memory NiTi alloy. Met Mater Int 25:1420–1427. https://doi.org/10.1007/s12540-019-00298-z

Dagdelen F, Balci E, Qader IN, Ozen E, Kok M, Kanca MS, Abdullah SS, Mohammed SS (2020) Influence of the Nb content on the microstructure and phase transformation properties of NiTiNb shape memory alloys. JOM 72:1664–1672. https://doi.org/10.1007/s11837-020-04026-6

Dong G, Gao Z (2016) Effect of heat treatment on the crystal structure, martensitic transformation and magnetic properties of Mn53Ni25Ga22 ferromagnetic shape memory alloy. J Magn Magn Mater 399:185–191. https://doi.org/10.1016/j.jmmm.2015.09.075

El-Bagoury N (2014) Microstructure and martensitic transformation and mechanical properties of cast Ni rich NiTiCo shape memory alloys. Mater Sci Technol 30:1795–1800. https://doi.org/10.1179/1743284713Y.0000000478

El-Bagoury N, Amin MA, Shokry H (2013) Microstructure and corrosion behavior of Ni52Ti48-xCox shape memory alloys in 1.0 M HCl solution. Int J Electrochem Sci 8:1246–1261

Elwindari N, Kurniawan B, Kurniawan C, Manaf A (2017) Microstructure and magnetic properties of optimally annealed Ni43Mn41Co5Sn11Heusler alloy. IOP Conf Ser Mater Sci Eng 196:012019. https://doi.org/10.1088/1757-899x/196/1/012019

Ercan E, Dagdelen F, Qader IN (2020) Effect of tantalum contents on transformation temperatures, thermal behaviors and microstructure of CuAlTa HTSMAs. J Therm Anal Calorim 139:29–36. https://doi.org/10.1007/s10973-019-08418-y

Fukushima K, Sano K, Kanomata T, Nishihara H, Furutani Y, Shishido T, Ito W, Umetsu RY et al (2009) Phase diagram of Fe-substituted Ni–Mn–Sn shape memory alloys. Scripta Mater 61:813–816. https://doi.org/10.1016/j.scriptamat.2009.07.003

GschneidnerJr KA, Pecharsky VK, Tsokol AO (2005) Recent developments in magnetocaloric materials. Rep Prog Phys 68:1479–1539. https://doi.org/10.1088/0034-4885/68/6/r04

Huang L, Cong DY, Ma L, Nie ZH, Wang MG, Wang ZL, Suo HL, Ren Y et al (2015) Large magnetic entropy change and magnetoresistance in a Ni41Co9Mn40Sn10 magnetic shape memory alloy. J Alloy Compd 647:1081–1085. https://doi.org/10.1016/j.jallcom.2015.06.175

Ito W, Imano Y, Kainuma R, Sutou Y, Oikawa K, Ishida K (2007) Martensitic and magnetic transformation behaviors in Heusler-type NiMnIn and NiCoMnIn Metamagnetic shape memory alloys. Metall Mater Trans A 38:759–766. https://doi.org/10.1007/s11661-007-9094-9

Kainuma R, Imano Y, Ito W, Morito H, Sutou Y, Oikawa K, Fujita A, Ishida K et al (2006a) Metamagnetic shape memory effect in a Heusler-type Ni43Co7Mn39Sn11 polycrystalline alloy. Appl Phys Lett 88:192513. https://doi.org/10.1063/1.2203211

Kainuma R, Imano Y, Ito W, Sutou Y, Morito H, Okamoto S, Kitakami O, Oikawa K et al (2006b) Magnetic-field-induced shape recovery by reverse phase transformation. Nature 439:957–960. https://doi.org/10.1038/nature04493

Kamila S (2013) Introduction, classification and applications of smart materials: an overview. Am J Appl Sci 10:876

Khalil-Allafi J, Dlouhy A, Eggeler G (2002) Ni4Ti3-precipitation during aging of NiTi shape memory alloys and its influence on martensitic phase transformations. Acta Mater 50:4255–4274. https://doi.org/10.1016/S1359-6454(02)00257-4

Khovaylo VV, Skokov KP, Gutfleisch O, Miki H, Takagi T, Kanomata T, Koledov VV, Shavrov VG et al (2010) Peculiarities of the magnetocaloric properties in Ni-Mn-Sn ferromagnetic shape memory alloys. Phys Rev B 81:214406. https://doi.org/10.1103/PhysRevB.81.214406

Kök M, Pirge G, Aydoğdu Y (2013) Isothermal oxidation study on NiMnGa ferromagnetic shape memory alloy at 600–1000° C. Appl Surf Sci 268:136–140

Kök M, Durğun SB, Özen E (2019a) Thermal analysis, crystal structure and magnetic properties of Cr-doped Ni–Mn–Sn high-temperature magnetic shape memory alloys. J Therm Anal Calorim 136:1147–1152. https://doi.org/10.1007/s10973-018-7823-5

Kök M, Qader IN, Mohammed SS, Öner E, Dağdelen F, Aydogdu Y (2019b) Thermal stability and some thermodynamics analysis of heat treated quaternary CuAlNiTa shape memory alloy. Mater Res Express 7:015702. https://doi.org/10.1088/2053-1591/ab5bef

Kök M, Zardawi HSA, Qader IN, Sait Kanca M (2019c) The effects of cobalt elements addition on Ti2Ni phases, thermodynamics parameters, crystal structure and transformation temperature of NiTi shape memory alloys. Eur Phys J plus 134:197. https://doi.org/10.1140/epjp/i2019-12570-9

Kök M, Al-Jaf AOA, Çirak ZD, Qader IN, Özen E (2020) Effects of heat treatment temperatures on phase transformation, thermodynamical parameters, crystal microstructure, and electrical resistivity of NiTiV shape memory alloy. J Therm Anal Calorim 139:3405–3413. https://doi.org/10.1007/s10973-019-08788-3

Lázpita P, Sasmaz M, Cesari E, Barandiarán JM, Gutiérrez J, Chernenko VA (2016) Martensitic transformation and magnetic field induced effects in Ni42Co8Mn39Sn11 metamagnetic shape memory alloy. Acta Mater 109:170–176. https://doi.org/10.1016/j.actamat.2016.02.046

Li C, Ruan H, Chen D, Li K, Guo D, Shao B (2018) Effect of heat treatment on the microstructure and properties of Ni based soft magnetic alloy. Microsc Res Tech 81:796–802. https://doi.org/10.1002/jemt.23038

Liu DM, Cong DY, Sun XM, Chen HY, Nie ZH, Chen Z, Zhang Y, Zhu C et al (2017) Low-hysteresis tensile superelasticity in a Ni-Co-Mn-Sn magnetic shape memory microwire. J Alloy Compd 728:655–658. https://doi.org/10.1016/j.jallcom.2017.09.055

Mañosa L, Moya X, Planes A, Krenke T, Acet M, Wassermann EF (2008) Ni–Mn-based magnetic shape memory alloys: Magnetic properties and martensitic transition. Mater Sci Eng A 481–482:49–56. https://doi.org/10.1016/j.msea.2007.01.178

Mishra SS, Yadava TP, Mukhopadhyay S, Yadav RM, Subrahmanyam VS, Mukhopadhyay NK, Srivastava ON (2015) Rapidly Quenched Ni45Fe5Mn40Sn10 Heusler Alloys. Mater Res 18:101–105. https://doi.org/10.1590/1516-1439.320814

Mohammed SS, Kok M, Qader IN, Kanca MS, Ercan E, Dağdelen F, Aydoğdu Y (2020) Influence of Ta additive into Cu84−x-Al13Ni3 (wt%) shape memory alloy produced by induction melting. Iranian J Sci Technol Trans Sci 44:1167–1175. https://doi.org/10.1007/s40995-020-00909-0

Otsuka K, Wayman CM (1999) Shape memory materials. Cambridge university press, Cambridge

Öztürk S, İçin K, Gençtürk M, Göbülük M, Svec P (2020) Effect of heat treatment process on the structural and soft magnetic properties of Fe38Co38Mo8B15Cu ribbons. J Non-Cryst Solids 527:119745

Qader IN, Kök M, Dağdelen F (2019) Effect of heat treatment on thermodynamics parameters, crystal and microstructure of (Cu-Al-Ni-Hf) shape memory alloy. Phys B 553:1–5. https://doi.org/10.1016/j.physb.2018.10.021

Qader IN, Ercan E, Faraj BAM, Kok M, Dagdelen F, Aydogdu Y (2020a) The influence of time-dependent aging process on the thermodynamic parameters and microstructures of quaternary Cu79–Al12–Ni4–Nb5 (wt%) shape memory alloy. Iranian J Sci Technol Trans Sci 44:903–910. https://doi.org/10.1007/s40995-020-00876-6

Qader IN, Kok M, Cirak ZD (2020b) The effects of substituting Sn for Ni on the thermal and some other characteristics of NiTiSn shape memory alloys. J Therm Anal Calorim 145:279–288. https://doi.org/10.1007/s10973-020-09758-w

Qader IN, Öner E, Kok M, Mohammed SS, Dağdelen F, Kanca MS, Aydoğdu Y (2020c) Mechanical and thermal behavior of Cu84−xAl13Ni3Hfx shape memory alloys. Iranian J Sci Technol Trans Sci 45:343–349. https://doi.org/10.1007/s40995-020-01008-w

Qu YH, Cong DY, Li SH, Gui WY, Nie ZH, Zhang MH, Ren Y, Wang YD (2018) Simultaneously achieved large reversible elastocaloric and magnetocaloric effects and their coupling in a magnetic shape memory alloy. Acta Mater 151:41–55. https://doi.org/10.1016/j.actamat.2018.03.031

Shen B, Sun J, Hu F, Zhang H, Cheng Z (2009) Recent progress in exploring magnetocaloric materials. Adv Mater 21:4545–4564. https://doi.org/10.1002/adma.200901072

Sutou Y, Imano Y, Koeda N, Omori T, Kainuma R, Ishida K, Oikawa K (2004) Magnetic and martensitic transformations of NiMnX(-X=In, Sn, Sb) ferromagnetic shape memory alloys. Appl Phys Lett 85:4358–4360. https://doi.org/10.1063/1.1808879

Tatar C, Yildirim Z (2017) Phase transformation kinetics and microstructure of NiTi shape memory alloy: effect of hydrostatic pressure. Bull Mater Sci 40:799–803. https://doi.org/10.1007/s12034-017-1413-1

Tatar C, Acar R, Qader IN (2020) Investigation of thermodynamic and microstructural characteristics of NiTiCu shape memory alloys produced by arc-melting method. Eur Phys J plus 135:311. https://doi.org/10.1140/epjp/s13360-020-00288-w

Yang Z, Cong DY, Huang L, Nie ZH, Sun XM, Zhang QH, Wang YD (2016) Large elastocaloric effect in a Ni–Co–Mn–Sn magnetic shape memory alloy. Mater Des 92:932–936. https://doi.org/10.1016/j.matdes.2015.12.118

Zimm C, Jastrab A, Sternberg A, Pecharsky V, Gschneidner K, Osborne M, Anderson I (1998) Description and performance of a near-room temperature magnetic refrigerator. In: Advances in cryogenic engineering. Springer, Boston, MA, pp 1759–1766. https://doi.org/10.1007/978-1-4757-9047-4_222